JOURNAL OF THERMOPHYSICS AND HEAT TRANSFER
Vol. 20, No. 4, October–December 2006

Technical Notes

TECHNICAL NOTES are short manuscripts describing new developments or important results of a preliminary nature. These Notes should not exceed 2500 words (where a figure or table counts as 200 words). Following informal review by the Editors, they may be published within a few months of the date of receipt. Style requirements are the same as for regular contributions (see inside back cover).

Application of Lumped-System Analysis to Layered Porous Cavities Heated from Below

M. J. Voon,* C. C. Ngo,† and F. C. Lai‡
University of Oklahoma, Norman, Oklahoma 73019

Nomenclature

c_p	=	heat capacity, J/kg · K
g	=	gravitational acceleration, m/s^2
H	=	height of cavity, m
h	=	heat transfer coefficient, W/m^2 · K
K	=	permeability, m^2
K_A	=	effective permeability of vertical layers, m^2
K_H	=	effective permeability of horizontal layers, m^2
k	=	effective thermal conductivity of porous medium, W/m · K
L	=	width of cavity, m
Nu	=	average Nusselt number, hH/k
Ra	=	Rayleigh number, $Kg\beta(T_h - T_c)H/\alpha\nu$
Ra_1	=	base Rayleigh number, $K_1 g\beta(T_h - T_c)H/\alpha_1\nu_1$
T	=	temperature, K
X, Y	=	dimensionless Cartesian coordinates, x/L and y/H, respectively
x, y	=	Cartesian coordinates, m
α	=	effective thermal diffusivity of porous medium, $k/(\rho c_p)_f$, [m^2/s]
β	=	thermal expansion coefficient, $(-1/\rho)(\partial\rho/\partial T)_p$, K^{-1}
θ	=	dimensionless temperature, $(T - T_c)/(T_h - T_c)$
ν	=	kinematic viscosity of fluid, m^2/s
ρ	=	fluid density, kg/m^3
Ψ	=	dimensionless stream function

Subscripts

c	=	cold wall
f	=	fluid
h	=	hot wall
i	=	index of sublayer, 1, 2, . . .

Presented as Paper 2005-0182 at the AIAA 43rd Aerospace Science Meeting, Reno, NV, 10–13 January 2005; received 28 January 2005; revision received 2 January 2006; accepted for publication 4 January 2006.

*Graduate Research Assistant, School of Aerospace and Mechanical Engineering; currently, Technical Coordinator, Shell Oil Company, Bintulu, Malaysia.

†Graduate Research Assistant, School of Aerospace and Mechanical Engineering.

‡Associate Professor, School of Aerospace and Mechanical Engineering; flai@ou.edu. Associate Fellow AIAA.

Introduction

HEAT transfer in porous media has received considerable attention in the past few decades because of its important applications in engineering. However, most previous studies have focused on homogenous porous media, whereas layered porous media, although encountered more frequently in applications, have received little attention. For stability analysis, Masuoka et al.[1] made the first study of the onset of thermal convection in a two-layer porous system. Their work was later extended by McKibbin and O'Sullivan[2] to multilayer systems. Rees and Riley[3] further extended the classical stability problem into a three-dimensional domain. For heat transfer analysis, Donaldson[4] reported the first numerical result of heat convection in a multilayer system. This was followed by Rana et al.[5] in numerical simulation of a geothermal reservoir using a layered porous model. Their results compared favorably with the field data obtained. For horizontal layers, heat transfer results have been presented by McKibbin[6] as well as McKibbin and Tyvand.[7,8] For vertical layers, Poulikakos and Bejan[9] as well as Lai and Kulacki[10] have studied the effects of permeability contrast and thermal conductivity ratio on natural convection in two- or three-layer porous systems.

For engineering applications where the heat transfer rate from layered porous cavities is the most important concern, a quick and accurate estimate of this value is often desirable. As such, the objective of the present study is to examine the feasibility of applying the lumped system analysis as proposed by Leong and Lai[11,12] to layered porous systems in the calculation of heat transfer rate. The proposed lumped system analysis uses an effective permeability to represent a layered porous medium and treat the medium as if it were homogeneous. As they suggested, an effective permeability defined by the arithmetic average should be used when the sublayers are oriented parallel to the primary heat flow direction. On the other hand, an effective permeability based on the harmonic mean should be used when the sublayers are perpendicular to the primary heat flow. Clearly, if the proposed method is applicable, it can significantly reduce the computational efforts when dealing with heat transfer problems in layered porous media.

Note that the present problem is different from those of previous studies[11,12] in that the cavities are heated from below, instead of vertical walls. In this case, if the lumped system analysis were applicable, one would obtain a better heat transfer prediction for cavities with vertical sublayers using an effective permeability based on the arithmetic mean. On the other hand, for cavities with horizontal sublayers, an effective permeability based on the harmonic mean should be used.

Formulation and Numerical Method

The geometry considered is a square cavity, $L = H$ (Fig. 1). The cavity walls are impermeable. The vertical walls are insulated, whereas the top and bottom walls are differentially heated at constant temperatures T_h and T_c (where $T_h > T_c$). The cavity consists of two or four sublayers of equal thickness but with distinct permeabilities. For the four-layer case, the permeabilities of these sublayers are alternating among the sublayers, that is, $K_1 = K_3$ and $K_2 = K_4$. It is assumed that the sublayers are saturated with the same fluid. The dimensionless governing equations based on Darcy's law are given by Leong and Lai,[11,12]

$$\frac{\partial^2\Psi_i}{\partial X^2} + \frac{\partial^2\Psi_i}{\partial Y^2} = -Ra_i\frac{\partial\theta_i}{\partial X} \tag{1}$$

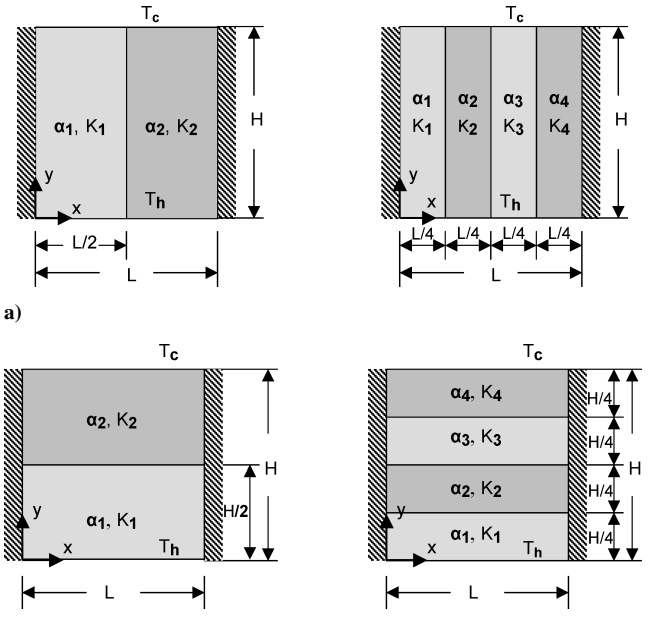

Fig. 1 Layered porous cavities with two or four sublayers subject to differential heating from below: a) vertical sublayers and b) horizontal sublayers.

$$\frac{\partial \Psi_i}{\partial Y}\frac{\partial \theta_i}{\partial X} - \frac{\partial \Psi_i}{\partial X}\frac{\partial \theta_i}{\partial Y} = \frac{\partial^2 \theta_i}{\partial X^2} + \frac{\partial^2 \theta_i}{\partial Y^2} \tag{2}$$

where $Ra_i = K_i g\beta(T_h - T_c)H/(\alpha_i \nu_i)$ and $\alpha_i = k_i/(\rho c_p)_f$.

In Eqs.(1) and (2), the subscript i refers to the individual sublayer in the cavity. In addition to the boundary conditions, interface conditions are required for the solution of the flow and temperature fields in the cavity. The interface conditions imposed are the continuity of mass, pressure, temperature, and heat flux across the interface. McKibbin and O'Sullivan[2] as well as Rana et al.[5] have justified the use of these conditions. For brevity, the dimensionless boundary and interface conditions are presented here only for a two-layer cavity, but can be extended to a four-layer case in a similar fashion.

For vertical sublayers,

$$X = 0, \qquad \Psi_1 = 0, \qquad \frac{\partial \theta_1}{\partial X} = 0 \tag{3a}$$

$$X = 1, \qquad \Psi_2 = 0, \qquad \frac{\partial \theta_2}{\partial X} = 0 \tag{3b}$$

$$X = \frac{1}{2}, \qquad \Psi_1 = \frac{\alpha_2}{\alpha_1}\Psi_2, \qquad \theta_1 = \theta_2$$

$$\frac{\partial \Psi_1}{\partial X} = \frac{K_1}{K_2}\frac{\alpha_2}{\alpha_1}\frac{\partial \Psi_2}{\partial X}, \qquad \frac{\partial \theta_1}{\partial X} = \frac{k_2}{k_1}\frac{\partial \theta_2}{\partial X} \tag{3c}$$

$$Y = 0, \qquad X < \frac{1}{2}, \qquad \Psi_1 = 0, \qquad \theta_1 = 1$$

$$X > \frac{1}{2}, \qquad \Psi_2 = 1, \qquad \theta_2 = 0 \tag{3d}$$

$$Y = 1, \qquad X < \frac{1}{2}, \qquad \Psi_1 = 0, \qquad \theta_1 = 0$$

$$X > \frac{1}{2}, \qquad \Psi_2 = 0, \qquad \theta_2 = 0 \tag{3e}$$

For horizontal sublayers,

$$X = 0, \qquad Y < \frac{1}{2}, \qquad \Psi_1 = 0, \qquad \frac{\partial \theta_1}{\partial X} = 0$$

$$Y > \frac{1}{2}, \qquad \Psi_2 = 0, \qquad \frac{\partial \theta_2}{\partial X} = 0 \tag{4a}$$

$$X = 1, \qquad Y < \frac{1}{2}, \qquad \Psi_1 = 0, \qquad \frac{\partial \theta_1}{\partial X} = 0$$

$$Y > \frac{1}{2}, \qquad \Psi_2 = 0, \qquad \frac{\partial \theta_2}{\partial X} = 0 \tag{4b}$$

$$Y = 0, \qquad \Psi_1 = 0, \qquad \theta_1 = 1 \tag{4c}$$

$$Y = 1, \qquad \Psi_2 = 0, \qquad \theta_2 = 0 \tag{4d}$$

$$Y = \frac{1}{2}, \qquad \Psi_1 = \frac{\alpha_2}{\alpha_1}\Psi_2, \qquad \frac{\partial \Psi_1}{\partial Y} = \frac{K_1}{K_2}\frac{\alpha_2}{\alpha_1}\frac{\partial \Psi_2}{\partial Y}$$

$$\theta_1 = \theta_2, \qquad \frac{\partial \theta_1}{\partial Y} = \frac{k_2}{k_1}\frac{\partial \theta_2}{\partial Y} \tag{4e}$$

Because the porous layers are saturated with the same fluid, thus, $\nu_1 = \nu_2$ and $\alpha_1 = \alpha_2$, the ratio of Rayleigh numbers can be obtained as

$$Ra_1/Ra_2 = K_1/K_2 \tag{5}$$

The interface conditions have been implemented using imaginary nodal points as described by Rana et al.[5]

The governing equations with the boundary and interface conditions were solved using a finite difference method. This method has been successfully employed by the authors for similar studies.[10–12] A uniform grid (101×101) with under- and overrelaxation was used for most of the calculations to ensure the efficiency and accuracy of the numerical results. When the solution converged, it was noticed that further refinement of the grid did not significantly improve the results. In addition, the present code has been validated against the previous results reported by Caltagirone[13] for a homogeneous porous cavity by setting $K_1/K_2 = 1$. The heat transfer results agree well with each other with a maximum discrepancy less than 5% for all of the Rayleigh numbers considered. For the present study, note that solutions for cavities with vertical sublayers require more iterations to converge than those with horizontal sublayers. In addition, it is more difficult to obtain converged solutions for cavities with $K_1/K_2 < 1$ than those of $K_1/K_2 > 1$. For some cases of $K_1/K_2 = 0.1$ and 0.01, a finer grid (201×201) was required. An overall energy balance has been performed in each calculation to further evaluate the accuracy of the results obtained. For the present study, the results are satisfied within 3%, whereas most are within 1%. The overall heat transfer is expressed in terms of the average Nusselt number at each vertical wall as given by

$$Nu = -\int_0^1 \left.\frac{\partial \theta}{\partial Y}\right|_{Y=0,\,1} \mathrm{d}X \tag{6}$$

Results and Discussion

For natural convection in a homogeneous porous layer heated from below, the flow and temperature fields are determined by the Rayleigh number and aspect ratio (see Refs. 13 and 14). For a square cavity, the onset of convection starts at $Ra = 40$ with a single cellular flow structure. With an increase in the Rayleigh number ($Ra > 100$), a transition to multicellular flow structure is observed. For natural convection in a layered porous cavity, heat transfer is further complicated by the presence of sublayers and their orientation, which becomes evident in the following discussion.

A. Cavities with Vertical Sublayers

The flowfields (in terms of stream function contours) in a cavity with four vertical sublayers are shown in Fig. 2 for various base Rayleigh numbers. Because the stream function contours are plotted with a constant interval, the closeness between two neighboring contour lines is directly proportional to the flow velocity. Because of the difficulty encountered in obtaining a converged solution at high base Rayleigh numbers for the case of $K_1/K_2 = 0.01$, its results are not presented. On the other hand, the flowfields for a homogeneous cavity are included for comparison. In general, the flow structure for a cavity with four sublayers bears some similarity to that of

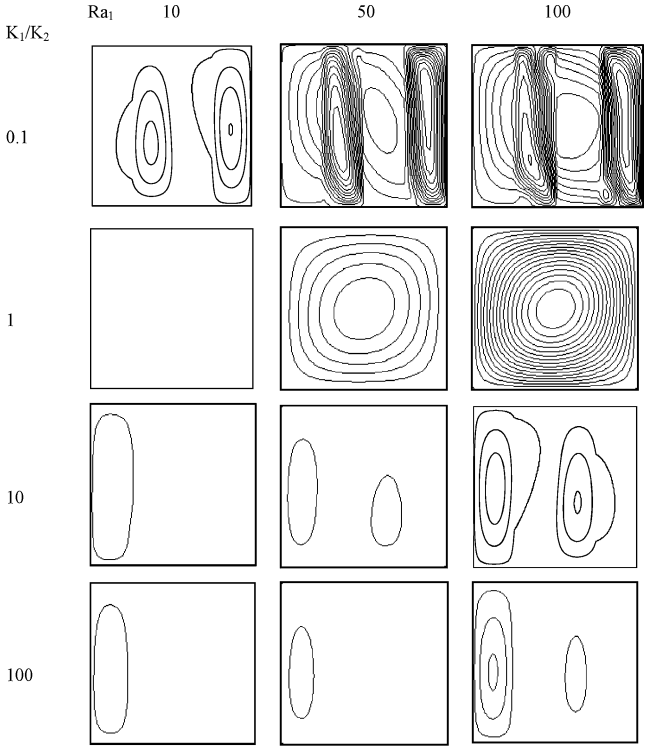

Fig. 2 Flowfields in square porous cavity with four vertical sublayers; $\Delta\Psi = 0.5$ for $K_1/K_2 \leq 1$ and $\Delta\Psi = 0.1$ for $K_1/K_2 > 1$ except $\Delta\Psi = 0.05$ for $K_1/K_2 = 10$ at $Ra_1 = 10$.

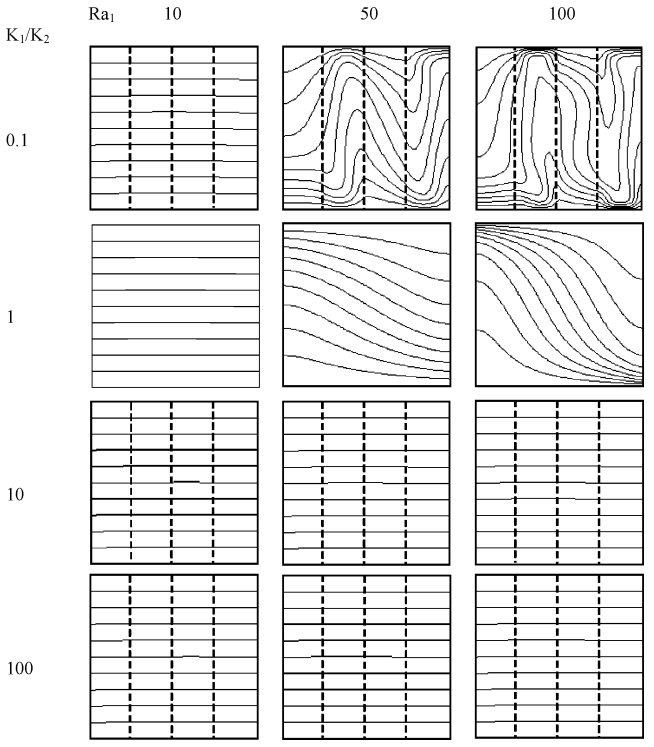

Fig. 3 Temperature fields in square porous cavity with four vertical sublayers; $\Delta\theta = 0.1$.

two vertical sublayers, only is more complicated by the presence of additional sublayers. Because of the difference in the permeability between two neighboring sublayers, the location of the interface can be easily identified by the abrupt change in the slope of streamlines. When the base Rayleigh number is small, that is, $Ra_1 = 10$, convection is not yet initiated in the homogeneous cavity. However, for layered cavities, convection starts in the more permeable sublayers, whereas fluid remains nearly stagnant in the less permeable sublayers. An increase in the base Rayleigh number leads to an increase in the strength of the convective cell. For $K_1/K_2 = 0.1$ and 10, this in turn prompts the flow penetration to a less permeable sublayer. The presence of a sandwiched less permeable sublayer breaks the convective cell into two portions. Thus, the sandwiched less permeable sublayer can be considered as a damper that simultaneously weakens and separates the convective flow. For $K_1/K_2 = 0.01$ (not shown) and 100, flow penetration to a less permeable sublayer is minimal. For these two cases, the less permeable sublayers act like an impermeable wall that has confined the convective flow to a limited space. As such, the strength of convective cells decreases with an increase in the permeability ratio. Note that the cavities for $K_1/K_2 = 0.1$ and 10 are geometrically in mirror symmetry. However, the flowfields shown in Fig. 2 may not appear so because they are presented in terms of the base Rayleigh number Ra_1. As such, the flowfield for $K_1/K_2 = 0.1$ at $Ra_1 = 10$ is not exactly a mirror image of that at $K_1/K_2 = 10$ and the same base Rayleigh number, but rather of that at $K_1/K_2 = 10$ and $Ra_1 = 100$. The slight difference in the mirror images between these two cases, that is, $K_1/K_2 = 0.1$ at $Ra_1 = 10$ and $K_1/K_2 = 10$ at $Ra_1 = 100$, is mainly due to the convergence criterion imposed.

The temperature fields (in terms of isotherm contours) in a cavity with four vertical sublayers are shown in Fig. 3 for various base Rayleigh numbers. The isotherm contours are also plotted with a constant interval, therefore, the closeness between two neighboring isotherms is directly proportional to the local heat flux. The dashed lines in Fig. 3 denote the locations of interface. The effect of permeability contrast is particularly visible for the cases of $K_1/K_2 = 0.1$, and it becomes even more apparent with the increase of base Rayleigh number. The heat transfer mode in each sublayer can be easily identified from the isotherm contours. The thermal stratification at a low base Rayleigh number, for example, $Ra_1 = 10$, indicates that heat transfer is driven by conduction. An increase in the base Rayleigh number produces plumelike isotherms in the cavities of $K_1/K_2 \leq 1$, which signifies a transition in the heat transfer mode from conduction to convection. For $K_1/K_2 > 1$, thermal stratification is maintained inside the cavities because of weak convection.

For $K_1/K_2 < 1$, the weak convective flow in the sandwiched less permeable sublayer, which is the result of flow penetration, prompts the transition of the heat transfer mode from conduction to convection at a lower base Rayleigh number. For $K_1/K_2 > 1$, it is clear that conduction remains the dominant heat transfer mode at low base Rayleigh numbers. This is confirmed by the presence of evenly distributed isotherms throughout the cavity. An increase in the base Rayleigh number causes only slight distortion to isotherms in the more permeable sublayer. The distortion of isotherms is an indication of weak convection. Regardless of the base Rayleigh number, conduction remains the primary heat transfer mode in the entire cavity for $K_1/K_2 > 1$.

For a given base Rayleigh number, the presence of sandwiched less permeable sublayer has created additional flow resistance that has to be overcome by the buoyancy-induced flow to sustain convection in the more permeable sublayers. This suggests that an increase in the number of sublayers suppresses the convection within the cavity.

B. Cavities with Horizontal Sublayers

For cavities with horizontal sublayers, the present results resemble those reported for partially heated layered porous cavities by Lai and Kulacki.[15] For $K_1/K_2 > 1$, the convective cell only appears in the more permeable sublayers (Fig. 4) when the base Rayleigh number is small, that is, $Ra_1 = 10$. With an increase in the base Rayleigh number, convective flow starts to penetrate the less permeable sublayer. This implies that conduction remains the main heat transfer mode inside the less permeable sublayer before flow penetration from the more permeable sublayer. The eye of the convective cell tends to shift toward the upper left corner of the cavity for $K_1/K_2 \leq 1$. On the other hand, for $K_1/K_2 > 1$, the eye of the

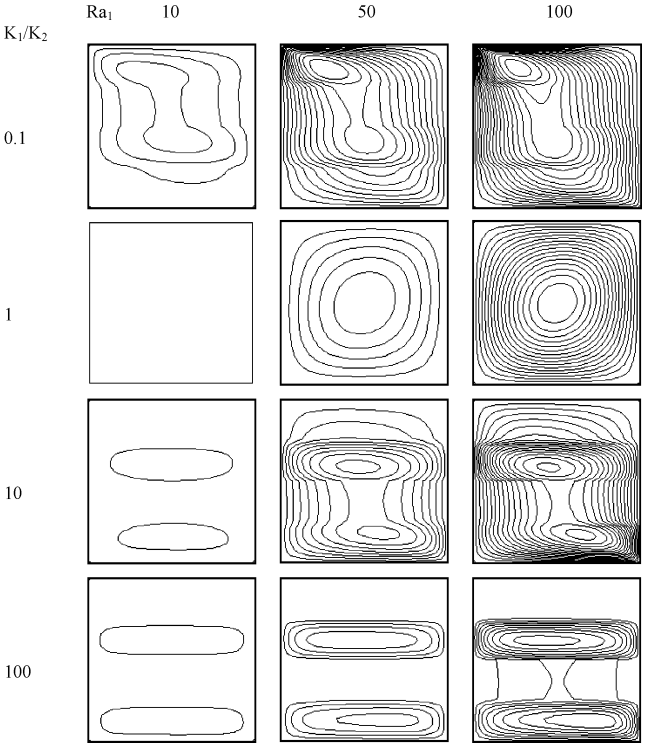

Fig. 4 Flowfields in square porous cavity with four horizontal sublayers; $\Delta\Psi = 0.5$ for $K_1/K_2 \leq 1$ and $\Delta\Psi = 0.1$ for $K_1/K_2 > 1$.

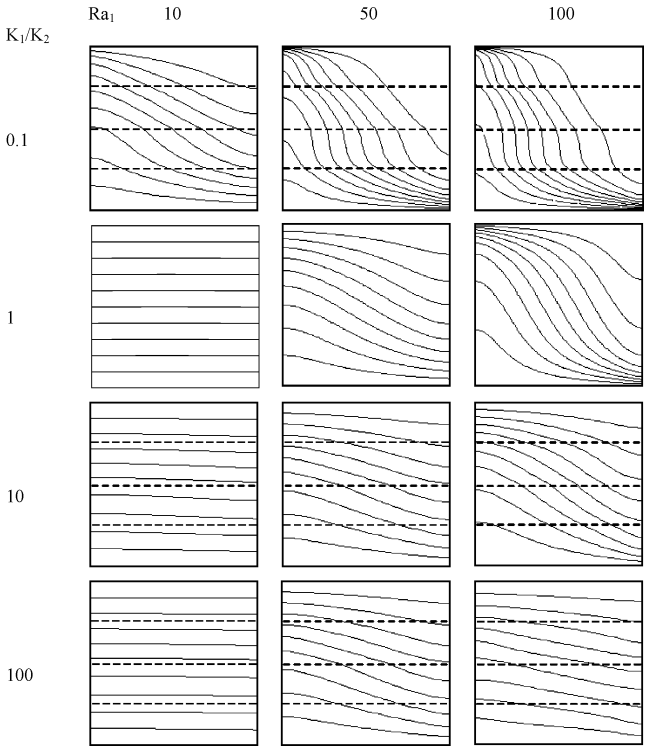

Fig. 5 Temperature fields in square porous cavity with four horizontal sublayers; $\Delta\theta = 0.1$.

convective cell is slightly shifted toward the bottom right corner of the cavity. The difference in the flow patterns between $K_1/K_2 < 1$ and $K_1/K_2 > 1$ is mainly caused by the heat transfer mode involved in each sublayer. For $K_1/K_2 = 0.1$, heat transfer from the bottom wall is first by conduction through the less permeable sublayer before it changes to convection in the more permeable sublayer. The density of streamlines in the less permeable sublayer indicates a weak convective flow in that sublayer. For $K_1/K_2 = 100$, the more permeable sublayer is at the bottom of the cavity. As such, heat transfer is mainly by convection in that sublayer. The upper less permeable sublayer acts like an impermeable wall, which confines the convective flow entirely to the more permeable sublayer at a low base Rayleigh number. When buoyancy is weak, no flow penetration into the upper (less permeable) sublayer is possible. Heat transfer in the less permeable sublayer, thus, becomes exclusively conduction at a low base Rayleigh number.

The heat transfer mode in each sublayer can be identified from Fig. 5. From the isotherm contours, one can tell that convection is the dominant heat transfer mode in each cavity with a low permeability ratio. For $K_1/K_2 = 0.1$, a thermal plume in the cavity is the evidence of such a claim. Because of the suppression of convective flow by additional sublayers, thermal plumes are less apparent in the four-sublayer cases than in the two-sublayer cases. The development of thermal boundary layers along the horizontal walls is further evidence of convection for the cases of $K_1/K_2 \leq 1$. An increase of the base Rayleigh number makes the thermal boundary layer along the bottom (hot) wall in the less permeable sublayer more apparent. For cavities with $K_1/K_2 > 1$, the nearly stratified isotherms (Fig. 5) imply that heat transfer is mainly driven by conduction at a low base Rayleigh number. The mode gradually changes to convection with an increase in the base Rayleigh number, and this can be observed from the rising of thermal plume. The transition in heat transfer mode is faster in the more permeable sublayer.

In general, flows in a cavity with four horizontal sublayers are stronger and more stable than those with four vertical sublayers. Unlike the cases of four vertical sublayers where convective cells are mostly confined to the more permeable sublayers, that is, local convection, convective cells in the present case spread over the entire cavity, that is, global convection. As such, the effect of sublayer orientation is more pronounced for cavities with four horizontal sublayers because heat has to transfer through all sublayers. In contrast, for cavities with four vertical sublayers, heat transfer is mainly by convection through the more permeable sublayers. Figure 4 shows that the convective flow in the sandwiched less permeable sublayers is mostly vertical, but becomes horizontal in other sublayers. With the aid of the buoyancy effect, heat transfer by flow penetration through all sublayers results in a higher heat transfer rate. An increase in the number of sublayers, however, weakens the convective flow in the cavity by breaking up the primary convective cell.

C. Heat Transfer Results

For heat transfer results, it is found that the average Nusselt number for $K_1/K_2 < 1$ is always greater than that of a homogeneous cavity, that is, $K_1/K_2 = 1$, whereas, it is always less than that of a homogeneous cavity for $K_1/K_2 > 1$. This is consistent with the results reported in previous studies.[10–12] To verify if the lumped-system analysis is applicable for the present problem, the Nusselt numbers obtained are expressed as a function of the Rayleigh number based on the effective permeability. For the present study, the vertical sublayers are parallel to the primary heat flow direction, whereas the horizontal sublayers are perpendicular to the heat flow direction. In the spirit of the lumped system analysis,[11,12] an effective permeability based on the arithmetic mean should be used for cavities with vertical sublayers and that of the harmonic mean should be used for cavities with horizontal sublayers. Therefore, for a cavity with vertical sublayers, its effective permeability is given by[11,12]

$$K_A = (K_1 + K_2)/2 \tag{7a}$$

and for a cavity with horizontal sublayers, it is given by

$$1/K_H = \tfrac{1}{2}(1/K_1 + 1/K_2) \tag{7b}$$

Because the resistance to convective heat transfer is inversely proportional to the sublayer permeability, Eq. (7a) represents a thermal circuit in parallel and Eq. (7b) represents that in series.

The heat transfer results are shown in Figs. 6 and 7 as a function of the effective Rayleigh number. For comparison, the results for

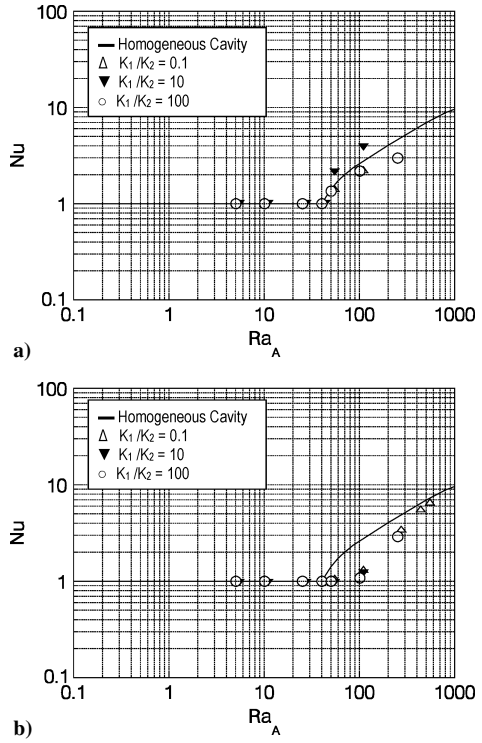

Fig. 6 Heat transfer results for porous cavity with a) two vertical sublayers and b) four vertical sublayers.

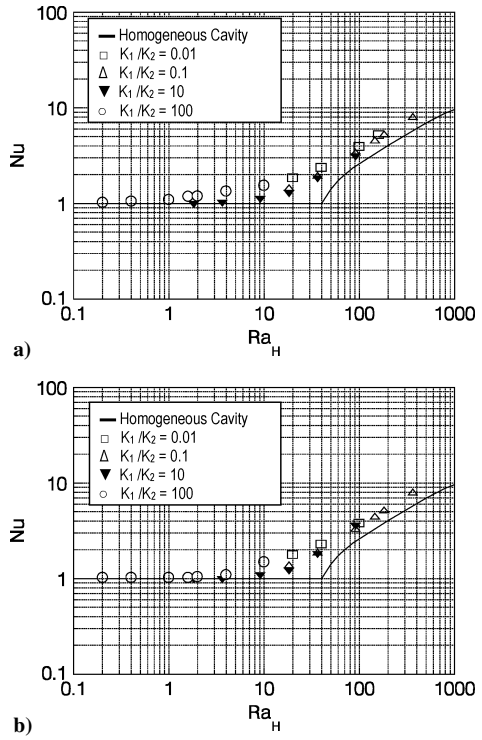

Fig. 7 Heat transfer results for porous cavity with a) two horizontal sublayers and b) four horizontal sublayers.

a homogeneous cavity are also included (as solid lines) in Figs. 6 and 7. For a homogeneous porous cavity, convection starts near $Ra = 40$ as predicted by theory (see Refs. 13 and 14). After the onset of convection ($Ra > 40$), Nusselt number increases with the Rayleigh number. However, notice that the slope of the Nusselt number is not uniform as the flow structure changes from a single cell to double cells when the Rayleigh number increases (see Ref. 14).

For cavities with two vertical sublayers, Fig. 6a shows that all data collapse nicely to the curve representing the homogeneous cavity if the effective permeability is based on the arithmetic mean. Similarly, for cavities with four vertical sublayers, it is observed that all data also collapse to a single curve when the effective permeability is based on the arithmetic mean (Fig. 6b). However, there is a discrepancy between the Nusselt number for a homogeneous cavity and that predicted by the lumped-system analysis. For cavities with four sublayers, the discrepancy is initially negligible at small Rayleigh numbers but grows to a maximum (about 50%) at $Ra_A = 100$ and then quickly diminishes as the Rayleigh number increases further. Note that if the effective permeability were based on the harmonic mean, data would become greatly scattered and no clear trend would be observed. Hence, one can conclude that the effective permeability based on the arithmetic mean allows a better prediction (although not perfect) in heat transfer for cavities with vertical sublayers.

For cavities with horizontal sublayers, one observes that all data fall nearly into a single curve when the effective permeability is based on the harmonic mean (Fig. 7). Again, if the effective permeability were based on the arithmetic mean, the data would have become more dispersed. Thus, observation has confirmed the previous report[11,12] that, for cavities with horizontal sublayers (in which the direction of heat flow is normal to the sublayers), the heat transfer results are better correlated with the Rayleigh number based on a harmonic effective permeability. However, also notice that the lumped-system analysis has generally over-predicted the homogeneous cavity Nusselt number. The discrepancy is negligible at small Rayleigh numbers but grows to a maximum (about 50%) at $Ra_H = 40$ and then decreases when the Rayleigh number becomes large ($Ra_H > 40$).

Conclusions

Natural convection in layered porous cavities heated from below has been numerically examined in this study as an extension to several earlier studies.[10–12] In addition, the present study has further examined the feasibility of using a lumped-system approach in the prediction of heat transfer results in layered porous cavities. For the present study, the discrepancy found between the actual results and those predicted by the lumped system in some cases is larger than those reported in the previous studies. This may be attributed to the nature of the problem presently considered, which is inherently more unstable than other heating conditions, and the flow and temperature fields of which are more susceptible to change with the Rayleigh number. However, it is observed that the Rayleigh numbers at which the discrepancy is a maximum fall outside the range of practical interest ($Ra > 100$). From this aspect, one can say with confidence that the lumped-system analysis is appropriate for most engineering applications involving layered porous media. In particular, the present study has further validated the basic principle in the determination of the effective permeability to be used in the lumped-system analysis. That is, for sublayers whose orientation is perpendicular to the primary heat flow, the effective permeability should be based on the harmonic average. On the other hand, for sublayers whose orientation is parallel to the primary heat flow, the effective permeability should be based on the arithmetic mean.

References

[1]Masuoka, T., Katsuhara, T., Nakazono, Y., and Isozaki, S., "Onset of Convection and Flow Patterns in a Porous Layer of Two Different Media," *Heat Transfer Japanese Research*, Vol. 7, No. 1, 1978, pp. 39–52.

[2]McKibbin, R., and O'Sullivan, M. J., "Onset of Convection in a Layered Porous Medium Heated from Below," *Journal of Fluid Mechanics*, Vol. 96, No. 2, 1980, pp. 375–393.

[3]Rees, D. A. S., and Riley, D. S., "The Three-Dimensional Stability of Finite-Amplitude Convection in a Layered Porous Medium Heated from Below," *Journal of Fluid Mechanics*, Vol. 211, Feb. 1990, pp. 437–461.

[4]Donaldson, I. G., "Temperature Gradients in the Upper Layers of the Earth's Crust Due to Convective Water Flows," *Journal of Geophysical Research*, Vol. 67, No. 9, 1962, pp. 3449–3459.

[5]Rana, R., Horne, R. N., and Cheng, P., "Natural Convection in a Multi-Layered Geothermal Reservoir," *Journal of Heat Transfer*, Vol. 101, No. 3, 1979, pp. 411–416.

[6]McKibbin, R., "Some Effects of Non-Homogeneity in the 'Water-Saturated Porous Layer' Model of a Geothermal Field," *Mathematics and Models in Engineering Science*, Dept. of Scientific and Industrial Research, Wellington, New Zealand, 1982, pp. 139–148.

[7]McKibbin, R., and Tyvand, P. A., "Thermal Convection in a Porous Medium Composed of Alternating Thick and Thin Layers," *International Journal of Heat and Mass Transfer*, Vol. 26, No. 5, 1983, pp. 761–780.

[8]McKibbin, R., and Tyvand, P. A., "Thermal Convection in a Porous Medium with Horizontal Cracks," *International Journal of Heat and Mass Transfer*, Vol. 27, No. 7, 1984, pp. 1007–1023.

[9]Poulikakos, D., and Bejan, A.,"Natural Convection in Vertically and Horizontally Layered Porous Media Heated from the Side," *International Journal of Heat and Mass Transfer*, Vol. 26, No. 12, 1983, pp. 1805–1814.

[10]Lai, F. C., and Kulacki, F. A., "Natural Convection across a Vertical Layered Porous Cavity," *International Journal of Heat and Mass Transfer*, Vol. 31, No. 6, 1988, pp. 1247–1260.

[11]Leong, J. C., and Lai, F. C., "Effective Permeability of a Layered Porous Cavity," *Journal of Heat Transfer*, Vol. 123, No. 3, 2001, pp. 512–519.

[12]Leong, J. C., and Lai, F. C., "Natural Convection in Rectangular Layered Porous Cavities," *Journal of Thermophysics and Heat Transfer*, Vol. 18, No. 4, 2004, pp. 457–463.

[13]Caltagirone, J. P., "Thermoconvective Instabilities in a Horizontal Layer," *Journal of Fluid Mechanics*, Vol. 72, No. 2, 1975, pp. 269–287.

[14]Bories, S., "Natural Convection in Porous Media," *Advances in Transport Phenomena in Porous Media*, edited by J. Bear and M. Y. Corapcioglu, NATO ASI Series E, No. 128, 1987, pp. 77–141.

[15]Lai, F. C., and Kulacki, F. A., "Natural Convection in Layered Porous Media Partially Heated from Below," *Heat Transfer in Geophysics and Geothermal System*, ASME HTD, Vol. 76, American Society of Mechanical Engineering, 1987, pp. 27–36.